J Mater Sci (2009) 44:939–944
DOI 10.1007/s10853-008-3205-x

Effects of Ga content on thermoelectric properties of P-type $Ba_8Ga_{16+x}Zn_3Ge_{27-x}$ type-I clathrates

Shu-kang Deng · Xin-feng Tang · Pei-zhi Yang · Ming Li

Received: 25 October 2008 / Accepted: 17 December 2008 / Published online: 15 January 2009
© Springer Science+Business Media, LLC 2009

Abstract P-type $Ba_8Ga_{16+x}Zn_3Ge_{27-x}$ ($x = 0.1$, 0.2, 0.3, and 0.4) type-I clathrates were synthesized by combining solid-state reaction with spark plasma sintering (SPS) technology. The effects of slight increase of Ga content on thermoelectric properties have been investigated. The results show that at room temperature the carrier concentration N_p of p-type $Ba_8Ga_{16+x}Zn_3Ge_{27-x}$ clathrates increases remarkably compared with that of $Ba_8Ga_{16}Zn_3Ge_{27}$ compound, which results in the increases of electrical conductivity although carrier mobility μ_H slightly decreases. The thermal conductivity κ of all samples increases with the increase of Ga content. $Ba_8Ga_{16.2}Zn_3Ge_{26.8}$ compound exhibits the highest *ZT* value of 0.43 at 700 K, which is increased by 13% compared with that of $Ba_8Ga_{16}Zn_3Ge_{27}$ compound.

Introduction

The performance of thermoelectric materials is usually evaluated by using the dimensionless thermoelectric figure of merit (*ZT*) defined as $ZT = \alpha^2\sigma T/\kappa$, where α, σ, κ, and T are the Seebeck coefficient, electrical conductivity, thermal conductivity, and absolute temperature, respectively. Type-I clathrate compounds, such as $Ba_8Ga_{16}Ge_{30}$, $Sr_8Ga_{16}Ge_{30}$, and $Eu_8Ga_{16}Ge_{30}$ [1–3] have been investigated intensively in recent years as promising thermoelectric materials due to their high electrical conductivity, large Seebeck coefficient, and low thermal conductivity.

Recently, the results of works investigated on Ge-based clathrates [2, 4–13] reveal that n-type Ge-based clathrates behave in a relatively higher *ZT* value compared with that of p-type clathrate [14–20]. However, the very low thermoelectric performance of p-type clathrate restricts its practical application. In our former work, Zn-doping p-type $Ba_8Ga_{16}Zn_xGe_{30-x}$ ($x = 2.4$, 2.6, 2.8, 3.0, 3.2) type-I clathrates have been synthesized successfully [21]. The results reveal that these compounds exhibit relatively higher Seebeck coefficient, and a maximum *ZT* of 0.38 is obtained for $Ba_8Ga_{16}Zn_3Ge_{27}$ compound, but the *ZT* value is relatively low due to the lower carrier concentration. Some research results [1, 22, 23] reveal that in Ge-based type-I clathrates, the Ga/Ge ratio can effect their thermoelectric transport properties remarkably. In this study, the thermoelectric performance of Zn-doping p-type Ge-based clathrate can be improved by slightly increasing Ga content, and the effects of Ga content on thermoelectric transport properties are investigated in order to develop high thermoelectric performance p-type clathrate.

Experimental details

Ge-based p-type $Ba_8Ga_{16+x}Zn_3Ge_{27-x}$ ($x = 0.1$, 0.2, 0.3, and 0.4) type-I clathrates were synthesized by combining solid-state reaction with spark plasma sintering (SPS) method. Stoichiometric amount of highly pure Ge (grain, 99.99%), Ga (ingot, 99.99%), Ba (ingot, 99.9%, Ba = 8.3, in order to compensate the loss during reaction), and Zn (grain, 99.99%) were placed in a graphite layer coated

---

S.-k. Deng (✉) · P.-z. Yang · M. Li
Education Ministry Key Laboratory of Renewable Energy
Advanced Materials and Manufacturing Technology,
Yunnan Normal University, Kunming 650092, China
e-mail: skdeng@163.com

X.-f. Tang
State Key Laboratory of Advanced Technology for Materials
Synthesis and Processing, Wuhan University of Technology,
Wuhan 430070, China

quartz tube. Then the quartz tube was sealed under the pressure of 1.0×10^{-2} Pa and was put into melting furnace. The sealed quartz tube was heated slowly to the temperature of 1,273 K at the heating rate of 5 K/min and was maintained at this temperature for 10 h, and then it was cooled in the furnace to the room temperature, The bulk samples with nearly 98% relative density were obtained by SPS with the sintering pressure, sintering temperature, and sintering time as 40 MPa, 1,023 K and 10 min, respectively. The constituent phase was characterized by X-ray diffraction (XRD, PANalytical X'Pert Pro X-ray diffraction). The morphology and element content was characterized by the back scattered electron imaging (BSI, JSM-5610LV) and electron probe microanalysis (EPMA, JXA8800). The Hall coefficient (R_H) under the room temperature was measured by Accent HL5500PC system using van der Pauw method. Electrical conductivity (σ) and Seebeck coefficient (α) were measured simultaneously using ZEM-1 apparatus in the temperature range from 300 to 870 K. The thermal conductivity κ in the temperature range from 300 K to 870 K was calculated from the equation of $\kappa = D \times Cp \times d$, where d is the density of the sample, the thermal diffusivity D and specific heat Cp were measured by a laser flash method (Shinkuriko: TC-7000).

Results and discussion

The composition and structure of samples

X-ray diffraction patterns of sample with $x = 0.4$ before SPS and after SPS are shown in Fig. 1 and the index parameters of crystal plane are also denoted. It can be seen from Fig. 1 that the XRD spectrum is a typical spectrum of single cubic structure with space group $pm\bar{3}n$, indicating that the prepared samples are type-I clathrates.

To further study the microstructure of sample, the BSI analysis and EPMA are carried out. Figure 2 shows the BSI morphology (a) and EPMA spectrum (b) of a sample with $x = 0.4$ after SPS. As shown in Fig. 2a, in addition to type-I clathrate, a microstructure consisting of trace Ge phase which cannot be detected by XRD is observed in the sample, and it can be assumed that the trace Ge cannot affect the thermoelectric transport properties. The actual composition of the sample is $Ba_{7.94}Ga_{16.37}Zn_{2.93}Ge_{26.11}$.

Electrical transport properties of p-type $Ba_8Ga_{16+x}Zn_3Ge_{27-x}$

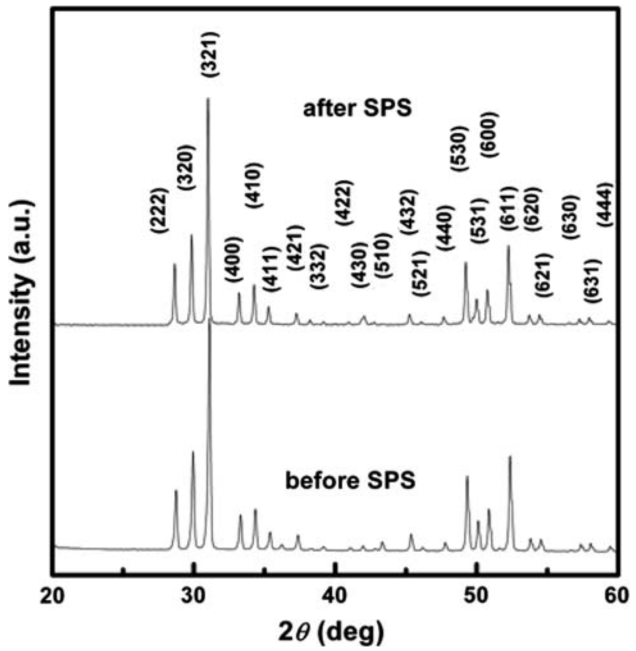

Fig. 1 XRD patterns of sample with $x = 0.4$ before SPS and after SPS

In Table 1, electrical conductivity σ, Hall coefficient R_H and carrier concentration N_p ($N_p = 1/qR_H$, q: positive electric charge) and actual composition obtained by EPMA, at the room temperature, are presented for $Ba_8Ga_{16+x}Zn_3Ge_{27-x}$ clathrates. The Hall coefficients R_H of all the samples are positive, which indicates the samples possess p-type conduction. The carrier concentration of p-type $Ba_8Ga_{16+x}Zn_3Ge_{27-x}$ is lower than that of n-type $Ba_8Ga_{16}Ge_{30}$ ($6.8 \times 10^{20}/cm^3$) [2]. The carrier concentration increases with the increase of Ga content, and the electrical conductivity increases accordingly although the slight decrease of carrier mobility with the increase of Ga content, especially for the sample with $x = 0.1$, the room temperature carrier concentration and the room temperature electrical conductivity increase sharply compared with $Ba_8Ga_{16}Zn_3Ge_{27}$ compound. From the Table 1 we can see that in the room temperature, the difference of the carrier concentration and the electrical conductivity between the adjacent two samples become inconspicuous with the increase of Ga content, indicating that it is an effective way to improve the electrical conductivity of p-type Ge-based clathrate by slightly increasing Ga content in a certain range. The carrier mobility of p-type $Ba_8Ga_{16+x}Zn_3Ge_{27-x}$ clathrates is higher than that of $Ba_8Ga_{16}Ge_{30}$, $Sr_8Ga_{16}Ge_{30}$, and $Eu_8Ga_{16}Ge_{30}$ n-type compound [2, 24, 25] at room temperature due to the reduction contribution of carrier scattering to carrier mobility caused by lower carrier concentration of p-type $Ba_8Ga_{16+x}Zn_3Ge_{27-x}$ clathrates.

Figure 3 shows the temperature dependence of electrical conductivity for p-type $Ba_8Ga_{16+x}Zn_3Ge_{27-x}$ samples with various Ga contents. The σ values increase with the increase of temperature, and reach their maximum value at about 700 K, and then decrease with increasing

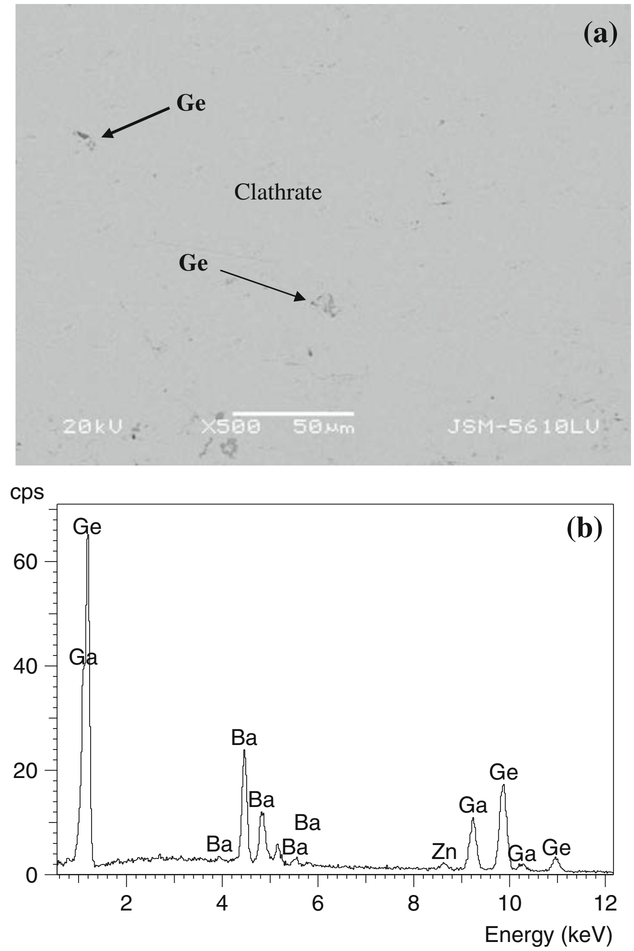

Fig. 2 **a** BSI and **b** EPMA spectrum of sample with $x = 0.4$ before SPS

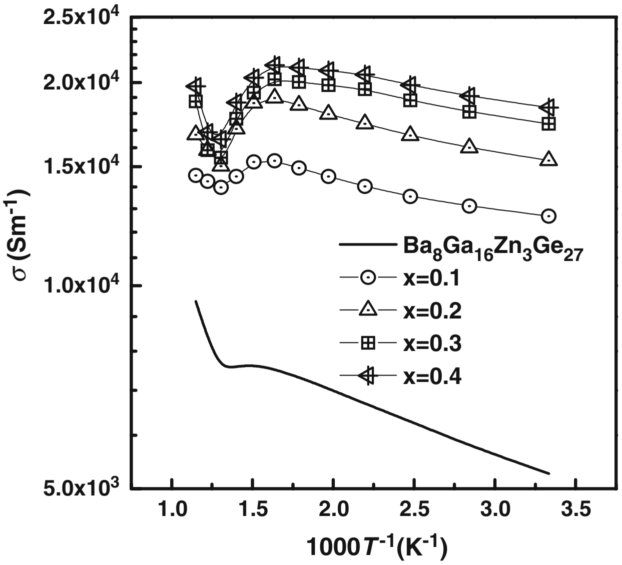

Fig. 3 Temperature dependence of electrical conductivity for $Ba_8Ga_{16+x}Zn_3Ge_{27-x}$ compounds

temperature. The process is followed by the increase with the temperature further increase after reaching their minimum value at about 800 K, which is a typical behavior of impurity semiconductor. The electrical conductivity increases with the increase of Ga content in the range of measured temperature. The difference of the electrical conductivity between the adjacent two samples become inconspicuous gradually with the increase of Ga content, which agree with the result of electrical conductivity in room temperature. The electrical conductivity of the sample with $x = 0.4$ reaches as large as 2.13×10^4 Sm^{-1} at about 600 K, and it is considerably enhanced compared with that of $Ba_8Ga_{16}Zn_3Ge_{27}$ compound at the same temperature. The temperature at which the intrinsic excitation takes place shift to low temperature may be due to the energy gap decrease with the increase of Ga content.

In $II_8III_{16}IV_{30}$ type-I clathrate, guest atoms donate electrons (as donor) to framework host atoms (as acceptor). Some (or all) of the electrons donated by guest atoms can be compensated by lone pairs formed in the cage structure through the elements of group-III or by dangling bonds formed around vacancies. In the present work, the lone pairs formed in the cage structure through the elements of group-III and group-IV increase with the increase of Ga content, and results in the increase of the hole carrier concentration with the increasing Ga content.

Figure 4 shows the Seebeck coefficient of p-type $Ba_8Ga_{16+x}Zn_3Ge_{27-x}$ clathrates as a function of temperature over the range from 300 to 870 K. The Seebeck coefficients of all samples are positive in the measured temperature range, which agrees with the results of Hall measurement. The value of α decreases with the increase of

Table 1 Some room temperature properties for $Ba_8Ga_{16+x}Zn_3Ge_{27-x}$ compounds under nominal composition

Nominal composition	Actual composition	Electrical conductivity σ (10^4 S/m)	Hall coefficient R_H (cm^3/C)	Carrier concentration N_p ($10^{19}/cm^3$)	Carrier mobility μ_H (cm^2/Vs)
$Ba_8Ga_{16}Zn_3Ge_{27}$	$Ba_{7.94}Ga_{15.79}Zn_{2.93}Ge_{26.21}$	0.56	+0.873	0.716	48.9
$Ba_8Ga_{16.1}Zn_3Ge_{26.9}$	$Ba_{8.07}Ga_{16.11}Zn_{2.91}Ge_{26.91}$	1.23	+0.243	2.53	30.1
$Ba_8Ga_{16.2}Zn_3Ge_{26.8}$	$Ba_{7.98}Ga_{16.21}Zn_{2.95}Ge_{26.74}$	1.52	+0.189	3.27	28.7
$Ba_8Ga_{16.3}Zn_3Ge_{26.7}$	$Ba_{8.03}Ga_{16.28}Zn_{2.98}Ge_{26.53}$	1.74	+0.143	4.31	24.9
$Ba_8Ga_{16.4}Zn_3Ge_{26.6}$	$Ba_{7.94}Ga_{16.37}Zn_{2.93}Ge_{26.11}$	1.82	+0.128	4.84	23.2

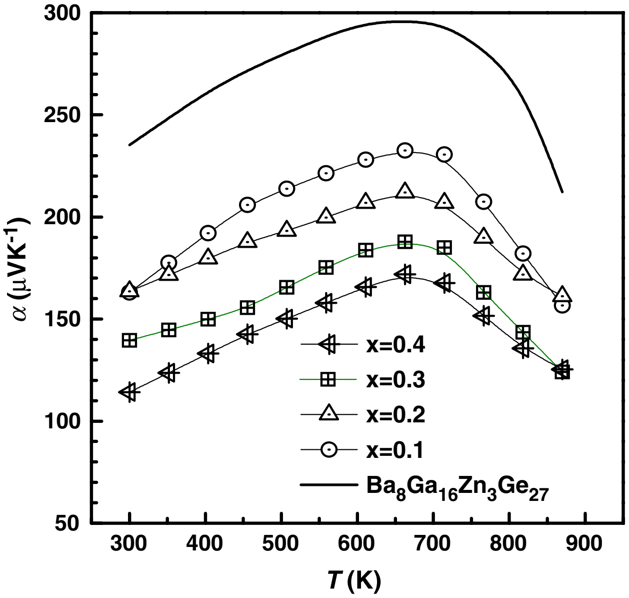

Fig. 4 Temperature dependence of Seebeck coefficient for $Ba_8Ga_{16+x}Zn_3Ge_{27-x}$ compounds

Ga content, and the temperature at which the Seebeck coefficient reaches its maximum value shift to lower temperature with the increase of Ga content due to the intrinsic excitation temperature decrease with the increase of Ga content, which is consistent with the changes of electrical conductivity. In general, the Seebeck coefficient decreases with the increase of carrier concentration. In this study, the carrier concentration of the sample increases with the increase of Ga content and consequently results in the decrease of the Seebeck coefficient. Nolas et al. [1] found that the effect of Ga/Ge ratio on the Seebeck coefficient α is distinctive, the absolute value of α increases with the increase of Ga/Ge ratio, which is opposite to our result. In this study, the main charge carrier is hole and it increase with the Ga/Ge ratios, but in the case of reference[1], the main charge carrier is electron and it decrease with the increase of Ga content, which results in the increase of α. The Seebeck coefficients of all samples increase with the increase of temperature and reach their maximum value at about 700 K and then gradually decrease with the further increase of temperature. The decrease of α in the high temperature range ($T > 700$ K) ascribes to the decreasing of absolute value of thermal electromotive force induced by the intrinsic excitation.

Thermal properties of $Ba_8Ga_{16+x}Zn_3Ge_{27-x}$

Figure 5 shows the thermal conductivity κ of p-type $Ba_8Ga_{16+x}Zn_3Ge_{27-x}$ clathrates as a function of temperature. The thermal conductivity κ of all samples increase with the increase of Ga content and reach their minimum value at about 650 K.

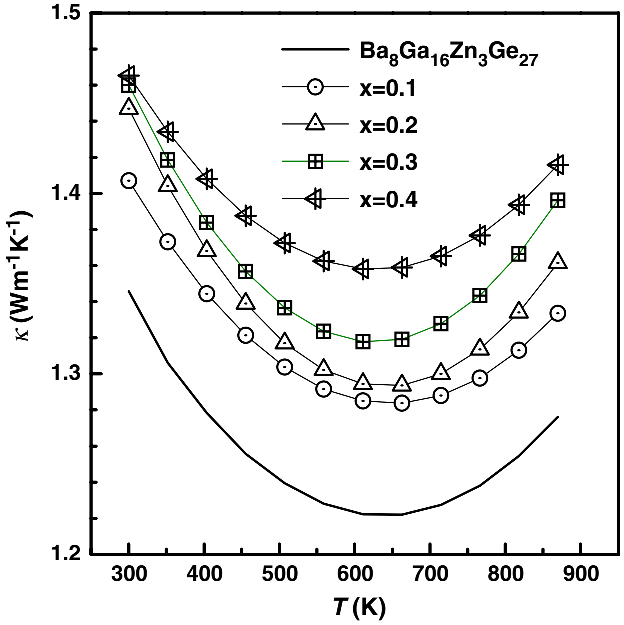

Fig. 5 Temperature dependence of thermal conductivity for $Ba_8Ga_{16+x}Zn_3Ge_{27-x}$ compounds

The thermal conductivity κ can be represented by the sum of a carrier component (κ_C) and a lattice component (κ_L) as

$$\kappa = \kappa_L + \kappa_C \tag{1}$$

The carrier component (κ_C) can be calculated using the Wiedenann–Franz law

$$\kappa_C = L\sigma T, \tag{2}$$

where L is the Lorenz number, σ is electrical conductivity, and T is absolute temperature. L can be calculated by Fermi level. In this study, $L = 2.4 \times 10^{-8}$ V^2/K^2 [2] is used to calculate κ_C. The value κ_C is very small for p-type $Ba_8Ga_{16}Zn_xGe_{27-x}$ clathrates because of the low electrical conductivity, and κ_L is a dominating part in the total thermal conductivity κ. Calculating indicates that the variety of Ga content has no apparent influence on the lattice thermal conductivity.

There are two kinds of cage in type-I clathrate structure, that is, pentagonal dodecahedra cage and hexakaidecahedra cage. The atoms vibration inside the cages cause phonon scattering to reduce lattice thermal conductivity, and then result in the reduction of total thermal conductivity κ. The atom displacement parameter (ADP) of atoms inside the hexakaidecahedra cage is larger than that of inside pentagonal dodecahedra because of the larger size of hexakaidecahedra cage [13]. The ADP of filling atoms is

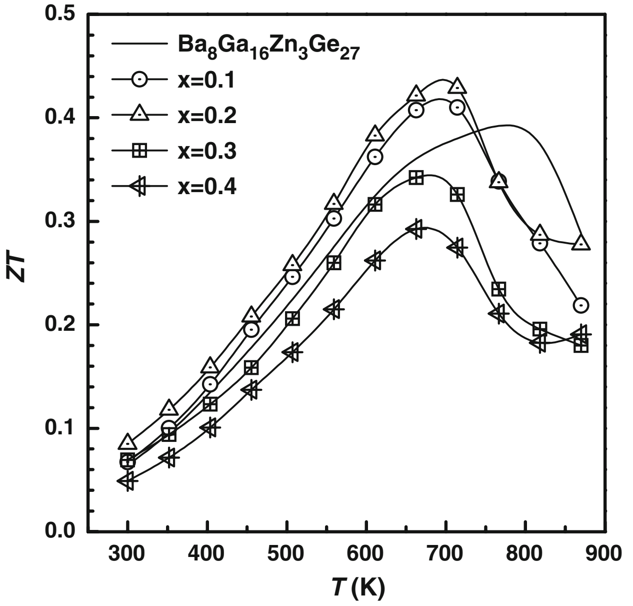

Fig. 6 Temperature dependence of ZT for $Ba_8Ga_{16+x}Zn_3Ge_{27-x}$ compounds

remarkably larger than that of framework in type-I clathrate, and the reduction of lattice conductivity κ_L is mainly caused by "rattling" of filling atoms; the vibration of framework atoms has no apparent influence on the lattice thermal conductivity [26].

Dimensionless thermoelectric figure of merit *ZT*

The dimensionless thermoelectric figure of merit ZT is calculated by using $ZT = \alpha^2\sigma T/\kappa$ from the measured electrical conductivity σ, the Seebeck coefficient α, and the thermal conductivity κ. Figure 6 shows the temperature dependence of ZT for p-type $Ba_8Ga_{16+x}Zn_3Ge_{27-x}$ samples. Of all the obtained p-type $Ba_8Ga_{16+x}Zn_3Ge_{27-x}$ samples, $Ba_8Ga_{16.2}Zn_3Ge_{26.9}$ shows the greatest ZT values in the measured temperature range. The maximum ZT value of 0.43 is obtained at about 700 K for this sample, and it is increased by 13% compared to that of $Ba_8Ga_{16}Zn_3Ge_{27}$ compound.

Conclusions

In this study, we mainly focus on enhancing carrier concentration of Zn-doping $Ba_8Ga_{16+x}Zn_3Ge_{27-x}$ type-I clathrates by increasing Ga content slightly and consequently to improve the figure of merit of p-type clathrate. The results show that the carrier concentration N_p of p-type $Ba_8Ga_{16+x}Zn_3Ge_{27-x}$ type-I clathrates increases remarkably compared with that of $Ba_8Ga_{16}Zn_3Ge_{27}$ compound which result in the increase of electrical conductivity remarkably although carrier mobility μ_H decreases slightly with the increase of Ga content. The thermal conductivity increases with the increasing of Ga content due to the increase of electrical conductivity. In all p-type $Ba_8Ga_{16+x}Zn_3Ge_{27-x}$ compounds, $Ba_8Ga_{16.2}Zn_3Ge_{26.8}$ exhibits the highest ZT value, it reaches 0.43 at 700 K, and it is increased by 13% compared with that of $Ba_8Ga_{16}Zn_3Ge_{27}$. It is an effective way to enhance the thermoelectric performance of p-type Zn-doping $Ba_8Ga_{16+x}Zn_3Ge_{27-x}$ type-I clathrates by slightly increasing the Ga content.

Acknowledgement This work is sponsored by the National Basic Research Program of China (Grant Nos. 2007CB607501 and 2007CB607503) and Yunnan Natural Science Fund (Grand No. 2008CD114).

References

1. Nolas GS, Cohn JL, Slack GA, Schujman SB (1998) Appl Phys Lett 73:178
2. Kuznetsov VL, Kuznetsova LA, Kaliazin AE, Rowe DM (2000) J Appl Phys 87:7871
3. Nolas GS, Weakley TJR, Cohn JL, Sharma R (2000) Phys Rev B 61:3845
4. Nolas GS (1999) Mater Res Soc Symp Proc 545:435
5. Paschen S, Carrillo-Cabrera W, Bentien A, Tran VH, Baenitz M, Grin Y, Steglich F (2001) Phys Rev B 64:214404
6. Bryan JD, Blake NP, Metiu H, Stucky GD, Iversen BB, Poulsen RD, Bentien A (2002) J Appl Phys 92:7281
7. Meng JF, Chandra Shekar NV, Badding JV, Nolas GS (2001) J Appl Phys 89:1730
8. Chakoumakos BC, Sales BC, Mandrus DG, Nolas GS (2000) J Alloys Compd 296:80
9. Cohn JL, Nolas GS, Fessatidis V, Metcalf TH, Slack GA (1999) Phys Rev Lett 82:779
10. Saramat A, Svensson G, Palmqvist AEC (2006) J Appl Phys 99:023708
11. Kim JH, Norihiko L, Okamoto KK, Katsushi T, Haruyuki I (2006) Acta Mater 54:2057
12. Chakoumakos BC, Sales BC, Mandrus DG, Nolas GS (2000) J Alloys Comp 296:80
13. Cai KF, Zhang LC, Lei Q, Muller E, Stiewe C (2006) Cryst Growth & Des 7:1797
14. Madsen GKH, Schwarz K, Blaha P, Singh DJ (2003) Phys Rev B 68:125212
15. Bentien A, Christensen M, Bryan JD, Sanchez A, Paschen S, Steglich F, Stucky GD, Iversen BB (2004) Phys Rev B 69:045107
16. Avila MA, Suekuni K, Umeo K, Takabatake T (2006) Phys B 383:124
17. Nolas GS, Slack GA, Schujman SB (2001) In: Tritt TM (ed) Semiconductors and semimetals. Academic Press Inc., New York, p 291
18. Kishimoto K, Akai K, Muraoka N, Koyanagi T, Matsuura M (2006) Appl Phys Lett 891:72106
19. Christensen M, Lock N, Overgaard J, Iversen BB (2006) J Am Chem Soc 128:15657
20. Latturner S, Bu X, Blake N, Metiu H, Stucky G (2000) J Solid State Chem 151:61
21. Deng SK, Tang XF, Zhang QJ (2007) J Appl Phys 102:043702

22. Pacheco V, Bentien A, Carrillo-Cabrera W, Paschen S, Steglich F, Grin Y (2005) Phys Rev B 71:165205
23. Bentien A, Pacheco V, Paschen S, Grin Y, Steglich F (2005) Phys Rev B 71:165206
24. Sales BC, Chakoumakos BC, Jin R, Thompson JR, Mandrus D (2001) Phys Rev B 63:245113
25. Uher C, Yang J, Hu S (1999) Mater Res Soc Symp Proc 54:247
26. Qiu L, Swainson IP, Nolas GS, White MA (2004) Phys Rev B 70:035208